

AD-A061 251

AIR FORCE FLIGHT DYNAMICS LAB WRIGHT-PATTERSON AFB OHIO

F/G 1/3

EJECTOR OPTIMIZATION.(U)

JUN 78 S H HASINGER

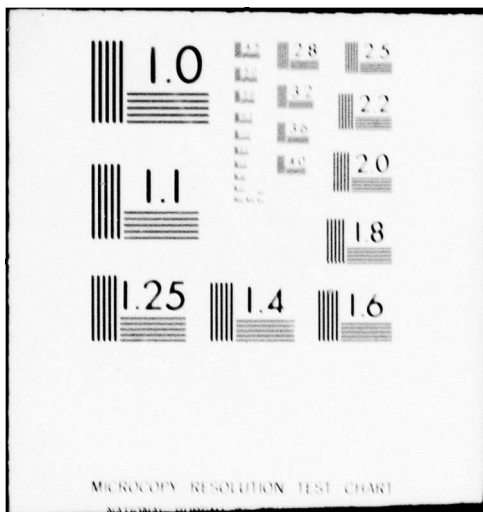
UNCLASSIFIED

AFFDL-TR-78-23

NL

/ OF /  
AD  
A061 251





AFFDL-TR-78-23

*P*  
B.S.

**LEVEL II**

AD A061251

**EJECTOR OPTIMIZATION**

Siegfried H. Hasinger  
Thermomechanics Branch  
Aero Mechanics Division

DDC  
NOV 16 1978  
*AS*

June 1978

TECHNICAL REPORT AFFDL-TR-78-23

Final Report for Period November 1976 - September 1977

Approved for public release; distribution unlimited.

AIR FORCE FLIGHT DYNAMICS LABORATORY  
AIR FORCE WRIGHT AERONAUTICAL LABORATORIES  
AIR FORCE SYSTEMS COMMAND  
WRIGHT-PATTERSON AIR FORCE BASE, OHIO 45433

78 10 27 023

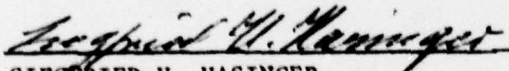
DDC FILE COPY

NOTICE

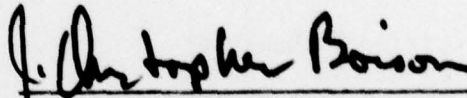
When Government drawings, specifications, or other data are used for any purpose other than in connection with a definitely related Government procurement operation, the United States Government thereby incurs no responsibility nor any obligation whatsoever; and the fact that the government may have formulated, furnished, or in any way supplied the said drawings, specifications, or other data, is not to be regarded by implication or otherwise as in any manner licensing the holder or any other person or corporation, or conveying any rights or permission to manufacture, use, or sell any patented invention that may in any way be related thereto.

This report has been reviewed by the Information Office (OI) and is releasable to the National Technical Information Service (NTIS). At NTIS, it will be available to the general public, including foreign nations.

This technical report has been reviewed and is approved for publication.



SIEGFRIED H. HASINGER  
Aerospace Engineer  
Aeromechanics Division



J. CHRISTOPHER BOISON  
Chief, Thermomechanics Branch  
Aeromechanics Division

FOR THE COMMANDER



MELVIN BUCK  
Acting Chief  
Aeromechanics Division

"If your address has changed, if you wish to be removed from our mailing list, or if the addressee is no longer employed by your organization please notify AFFDL/FXE, W-PAFB, OH 45433 to help us maintain a current mailing list".

Copies of this report should not be returned unless return is required by security considerations, contractual obligations, or notice on a specific document.



SECURITY CLASSIFICATION OF THIS PAGE (When Data Entered)

| REPORT DOCUMENTATION PAGE  |                       | READ INSTRUCTIONS<br>BEFORE COMPLETING FORM  |  |
|--|-----------------------|--|--|
| 1. REPORT NUMBER<br>AFFDL-TR-78-23   | 2. GOVT ACCESSION NO. | 3. RECIPIENT'S CATALOG NUMBER  |  |
| 4. TITLE (and Subtitle)<br>EJECTOR OPTIMIZATION,   |                       | 5. TYPE OF REPORT & PERIOD COVERED<br>Final Report,<br>Nov 76-Sept 77,   |  |
| 7. AUTHOR(s)<br>Siegfried H. Hasinger  |                       | 8. CONTRACT OR GRANT NUMBER(s)   |  |
| 9. PERFORMING ORGANIZATION NAME AND ADDRESS<br>Air Force Flight Dynamics Laboratory (AFFDL/FXE)<br>Air Force Wright Aeronautical Laboratories, AFSC<br>Wright-Patterson Air Force Base, Ohio 45433   |                       | 10. PROGRAM ELEMENT, PROJECT, TASK<br>AREA & WORK UNIT NUMBERS<br>Project 2307 1744<br>Task 230704<br>Work Unit 23070426 |  |
| 11. CONTROLLING OFFICE NAME AND ADDRESS<br>Air Force Flight Dynamics Laboratory (AFFDL/FX)<br>Air Force Wright Aeronautical Laboratories, AFSC<br>Wright-Patterson Air Force Base, Ohio 45433  |                       | 12. REPORT DATE<br>June 78   |  |
| 14. MONITORING AGENCY NAME & ADDRESS (if different from Controlling Office)<br>1253p.  |                       | 13. NUMBER OF PAGES<br>52  |  |
|  |                       | 15. SECURITY CLASS. (of this report)<br>Unclassified   |  |
|  |                       | 15a. DECLASSIFICATION/DOWNGRADING<br>SCHEDULE N/A  |  |
| 16. DISTRIBUTION STATEMENT (of this Report)<br>Approved for public release; distribution unlimited   |                       |  |  |
| 17. DISTRIBUTION STATEMENT (of the abstract entered in Block 20, if different from Report)   |                       |  |  |
| 18. SUPPLEMENTARY NOTES  |                       |  |  |
| 19. KEY WORDS (Continue on reverse side if necessary and identify by block number)<br>Ejector Optimization Analysis<br>Ejector Optimization Experiments<br>Supersonic Mixing<br>Flow Density Parameter<br>Supersonic Diffusion   |                       |  |  |
| 20. ABSTRACT (Continue on reverse side if necessary and identify by block number)<br>The ejector optimization process, reported in Reference 1 and tested in Reference 2, has been amended to include supersonic mixing. Several examples of ejector optimization have been calculated. Two of these examples have been checked experimentally. In one case for a pressure ratio of 3.1 and a mass flow ratio of 2.2 with air as operating media, experiment and analysis are in good agreement. For the other case with helium as secondary medium, the predicted optimum performance could not be reached, although operation not too far from |                       |  |  |

DD FORM 1 JAN 73 1473

EDITION OF 1 NOV 65 IS OBSOLETE

SECURITY CLASSIFICATION OF THIS PAGE (When Data Entered)

012 070

LB

## 20. Abstract (Continued)

optimum is in good agreement with the analysis. Mixing difficulties near the optimum point are apparently responsible for the discrepancies. A flow density plot has been introduced for a graphic interpretation of ejector operations. It shows that optimization brings the flow density at the mixing section exit to a maximum and that transition from subsonic to supersonic mixing, which is generally a requirement for optimization, occurs only after constant pressure mixing has been established.

FOREWORD

This report concludes the investigations on ejectors carried out under Work Unit No 23070426 of Project 2307 in the Thermomechanics Branch, Aeromechanics Division, Flight Dynamic Laboratory, from November 1976 to September 1977. Earlier reports are ARL TR-75-0205, "Performance Characteristics of Ejector Devices," June 1975, and AFFDL-TR-77-38, "Comparison of Experiment and Analysis for a High Primary Mach Number Ejector," May 1977.

*AD15040  
AD42 555*

Special thanks go to Captain David K. Miller, Technical Manager, Gas Energetics Group, Thermomechanics Branch, for his great interest in this investigation and for his many suggestions on the subject, and to Mr. Howard Toms for his most skillful completion of the experimental program.

|  |   |
|--|---|
| ACCESSION for  |   |
| NTIS   | White Section <input checked="" type="checkbox"/> |
| DDC  | Buff Section <input type="checkbox"/>             |
| UNANNOUNCED  | <input type="checkbox"/>                          |
| JUSTIFICATION  |   |
| BY   |   |
| DISTRIBUTION/AVAILABILITY CODES                                    |   |
| Circ. <input type="checkbox"/> or SPECIAL <input type="checkbox"/> |   |
| <i>A</i>   |   |



## TABLE OF CONTENTS

| SECTION   | PAGE |
|---|------|
| I INTRODUCTION  | 1    |
| II GENERAL ASPECTS OF EJECTOR OPTIMIZATION                            | 2    |
| III ANALYSIS OF OPTIMIZATION  | 4    |
| 1. Basic Process  | 4    |
| 2. Supersonic Solution of the Ejector Equations                       | 5    |
| 3. Supersonic Diffusion   | 6    |
| 4. Pressure Rise Parameter  | 7    |
| 5. Primary Supply Pressure  | 7    |
| IV OPTIMIZATION EXAMPLES  | 9    |
| 1. Analytic Results   | 9    |
| 2. Optimization Experiments   | 11   |
| V EJECTOR OPERATION IN TERMS OF THE FLOW DENSITY<br>PARAMETER         | 16   |
| 1. Flow Density Parameter   | 16   |
| 2. The Flow Density Plot  | 18   |
| 3. Typical Operating Conditions                                       | 19   |
| 4. Optimum Performance  | 23   |
| VI CONCLUSION   | 26   |
| APPENDIX: CALCULATOR PROGRAMS AND DERIVATIONS                         | 27   |
| 1. Equations for Calculating an Ejector Performance<br>Characteristic | 27   |
| 2. Equations for Calculating an Optimization Diagram                  | 31   |
| 3. Interpretation of the Flow Density Parameter                       | 34   |
| 4. Introduction of a Pressure Parameter in Figure 9                   | 36   |
| REFERENCES  | 37   |

PRECEDING PAGE BLANK

## LIST OF SYMBOLS

|              |   |
|--------------|---|
| $m$          | mass flow rate  |
| $v$          | flow velocity   |
| $\rho$       | mass density  |
| $A$          | flow cross section  |
| $a$          | sonic speed   |
| $\gamma$     | ratio of specific heats   |
| $R$          | gas constant  |
| $T$          | abs static temperature  |
| $p$          | static pressure   |
| $M$          | Mach number   |
| $c_f$        | pipe friction coefficient   |
| $L/D$        | length-diameter ratio of mixing section   |
| $t$          | mixing section taper (ratio of exit to inlet crosssectional area of mixing section)                     |
| $i$          | pressure distribution factor (for definition see Eq 37 of Ref 1) taken as 0.8 in this report            |
| $\eta_{pol}$ | polytropic subsonic diffuser efficiency   |
| $f$          | factor used as iteration criterion for solving the ejector equation (for definition see Eq 46 of Ref 1) |
| $c_p$        | specific heat at constant pressure  |
| $E$          | flow density parameter (Sect V-1)   |
| $\tau$       | factor to account for wall pressure forces (Sect V-1)   |

Indices

|         |                                       |
|---------|---------------------------------------|
| $p$     | refers to primary ejector medium      |
| $s$     | refers to secondary ejector medium    |
| $Ex$    | refers to ejector exit                |
| $Ex-m$  | refers to mixing section exit         |
| $Ex-d$  | refers to supersonic diffuser exit    |
| $Ref$   | refers to reference layout of ejector |
| $( )_o$ | indicates stagnation conditions       |



## SECTION I

## INTRODUCTION

This report supplements the investigations on ejector optimization presented in References 1 and 2. Reference 1 provided an analytical scheme for optimizing ejectors, considering only the subsonic mixing mode, i.e., the case in which the mixing section exit Mach number is subsonic. Reference 2 showed from experiments that for high primary Mach numbers the supersonic mixing mode becomes the only one possible for the optimized ejector. The present report analyzes the optimization with supersonic mixing and interprets optimization in terms of a flow density parameter. New experiments on ejector optimization are also described.

## SECTION II

## GENERAL ASPECTS OF EJECTOR OPTIMIZATION

The implications of the ejector analysis used in the present investigation and originally derived in Reference 1 are given first. The underlying flow scheme is shown in Figure 1.\* It involves three principle parts: mixing section, supersonic diffuser, and subsonic diffuser. Primary and secondary flow are assumed to have the same static pressure at the inlet to the mixing section. Primary and secondary flow are also assumed to be completely mixed at the mixing section exit. Details of the mixing process do not enter the analysis, and the flow conditions before and after mixing are related to each other by the conservation requirements for mass, momentum, and energy. Wall friction in the mixing section and supersonic diffuser is accounted for in terms of the common wall friction coefficient. Losses in the subsonic diffuser are covered by a diffuser efficiency. Ejector length dimensions do not enter the analysis except in an indirect manner for determining flow losses due to wall friction. All flow conditions considered are assumed to be one-dimensional.

The ejector analysis allows one to relate the ejector performance, given by the ejector pressure ratio  $(p_{Ex})_0/(p_s)_0$  (total exit to total secondary inlet pressure), and the ejector mass flow ratio  $m_p/m_s$  to the mixing section geometry, given by its principle cross-sectional areas. In more explicit terms, the ejector performance can be related to the three magnitudes: primary Mach number, inlet area ratio of primary to secondary flow, and area reduction ratio of the mixing section.

\*Figures are located at end of report.

Optimization of an ejector layout amounts to finding the most advantageous combination of the above-listed magnitudes, in particular, the combination which requires a minimum primary supply pressure to achieve a given ejector performance.

Figure 2 demonstrates that optimum operating conditions can be recognized in the performance characteristic of an ejector. In this figure, which applies to a specific ejector geometry, the secondary Mach number is plotted against the primary Mach number, with the ejector pressure ratio and the mass flow ratio appearing as parameters (for equations, see Appendix). In this characteristic, one sees that a given pressure ratio curve and a given mass flow ratio curve either cross each other twice, touch each other or never cross. For a given ejector pressure ratio, the mass flow ratio can obviously be reduced to a minimum if an operating point is chosen where both kind of curves become tangent to each other. Such tangent points represent optimum conditions, since a certain pressure ratio is obtained with a minimum of primary mass flow.

All tangent points in Figure 2 are connected by the dashed line (optimum line) in the upper right-hand corner of the figure. To the left, the dashed line approaches the "choking" line of the characteristic. Beyond this line no ejector operation is possible. Along this line the mixed flow obtains the highest possible flow density. Since the flow density after mixing is a direct measure for the effectiveness of the mixing process, the line of the highest density represents another location of preferred operating conditions. Apparently, the "best" optimum in Figure 2 must occur where the optimum line and the choking line meet or come at least close to each other.

The above discussion indicates that the performance which is best suited for a given ejector can be readily found from a performance characteristic as shown in Figure 2. The reversed case, which requires one to find the optimum geometry for a given performance and which is the subject of the present optimization process, is much more involved as we will see in the following section.



SECTION III  
ANALYSIS OF THE OPTIMIZATION

1. BASIC PROCESS

The basic relations for the optimization have been given in Reference 1. The Appendix of this report shows the equations in their sequence as they enter the calculation process. A short outline of the process is as follows:

a) With the ejector pressure ratio and the mass flow ratio given, the ejector equations are solved for the primary Mach number and the inlet area ratio. The area reduction of the mixing section and the character of the pressure distribution during mixing are thereby treated as constants. The secondary Mach number is maintained as an independent variable.

b) By plotting the primary Mach number against the secondary Mach number for a number of mixing section reduction ratios one finds graphically the minimum primary Mach number required for the given ejector task. The examples given in Reference 1 considered only the subsonic solution of the ejector equations.

This basic process is amended here as follows:

1) The supersonic solution of the ejector equations instead of the subsonic one is used.

2) The supersonic diffusion is treated as a process by itself separated from mixing and subsonic diffusion.

3) A new parameter characterizing the pressure increase during mixing is introduced making constant pressure mixing a special case of this parameter.

4) Lines of constant primary supply pressure are introduced in the performance diagram.

These new features will be discussed below.

## 2. SUPERSONIC SOLUTION OF THE EJECTOR EQUATIONS

As mentioned before, Reference 2 made it clear that supersonic mixing is an inherent feature of an optimized ejector with a high primary Mach number. The conditions necessary for the existence of supersonic mixing are discussed in Section V. Analytically the supersonic solution is obtained by taking the negative sign for the square root in Equation 22c in Reference 1 (Equation 13 in Appendix).

The choice of the solution is not necessarily connected to the prevailing type of mixing. By including the supersonic diffusion into the mixing process as a normal shock taking place at the end of the mixing section, the exit flow is always subsonic. This system of calculation was actually used in References 1 and 2. The distinction between subsonic and supersonic mixing is then shifted to the assumptions made for the shape of the pressure distribution along the mixing section. The analysis characterizes this shape by the pressure distribution factor  $i$  (Reference 1). This factor does not predetermine any pressures. Its basic purpose is to facilitate the integration of the wall pressure forces in flow direction. Since the shape of the pressure distribution has an essential influence on these forces, this factor becomes also a shape factor. By definition this factor is 1 if the pressure in the mixing section rises proportionally with the change in cross-section area of the mixing section. For a conical mixing section, this means in general that the pressure rises nearly in a straight line along the mixing section. A factor of zero implies zero pressure rise during mixing, and thus zero wall forces. A sudden pressure rise, as a normal shock would produce, at the end of the mixing section does not change the wall forces in flow direction. Therefore a pressure distribution factor zero as used in References 1 and 2 characterizes constant pressure mixing with the supersonic exit Mach number converted to subsonic in a normal shock at the mixing section exit. For  $i = 1$  the pressure rises as indicated in a nearly straight line, characterizing a mixing process where shock diffusion occurs during mixing, resulting



in a subsonic mixing section exit Mach number. Values of  $i$  between 0 and 1 cover then all cases where the pressure rises partly during mixing and partly during the supersonic diffusion.

For the present calculations, the supersonic diffusion after mixing is treated as a separate process. This has distinct advantages for dealing with the diffusion process (see Section III.3). It also greatly simplifies the assumptions to be made for the factor  $i$ , since it must only account for the character of the pressure distribution during mixing. In approaching constant pressure mixing, a shape factor becomes irrelevant and a factor of 1 gives practically the same result as a factor of zero, which is obvious since with a constant pressure distribution the wall forces become zero independent of the shape of the pressure distribution. In the case of supersonic mixing, experience shows that the shape of the distribution curve is quite generally that of a somewhat sagging line characterized by an  $i$ -factor somewhat less than 1. Therefore, the pressure distribution factor can be considered a constant with good approximation. The present calculations, which use exclusively the supersonic solution, assume in all cases a value of .8 for the pressure distribution factor.

### 3. SUPERSONIC DIFFUSION

For the convenience of the calculations, the supersonic diffusion is treated as an ejector process, with the primary and secondary Mach number being equal. The advantage of this approach is that wall friction losses can be readily included. In addition, this approach covers the flow in a duct in a general manner, and no change in the relations is necessary to distinguish between subsonic or supersonic inlet flow. Only constant area diffusion is considered. This calculation process yields the downstream Mach number as the subsonic solution of the ejector equations. The pressure ratio across the shock is also readily obtained. The wall friction losses are computed using the downstream Mach number as reference Mach number since in a pseudo-shock process the diffuser wall is almost exclusively exposed to subsonic conditions. The actual sequence of

equations for treating the supersonic diffusion with the ejector equations is given in the Appendix (Equations 14 to 17).

#### 4. PRESSURE RISE PARAMETER

This parameter has been introduced to provide a general identification of the mixing cases. Constant pressure mixing is a special case in this scheme. The definition of this parameter is

$$\pi = \frac{P_{EX-m} - P_S}{P_{EX-d} - P_S}$$

i.e., it is the ratio of the static pressure rise during mixing over the static pressure rise during mixing and supersonic diffusion. For the analysis the parameter is written in the form

$$\pi = \frac{\frac{P_{EX-m}}{P_S} - 1}{\frac{P_{EX-d}}{P_{EX-m}} \cdot \frac{P_{EX-m}}{P_S} - 1}$$

All pressure ratios occurring in this relation are readily obtained from the analysis. For constant pressure mixing,  $\pi$  becomes zero. It becomes negative in case of a decreasing pressure during mixing. This parameter can be conveniently used to show the influence of the pressure rise during mixing on the ejector optimization (Section IV 1a).

#### 5. PRIMARY SUPPLY PRESSURE

The primary supply pressure can be expressed in the following way:

$$(p_p)_0 = \left[ \frac{(p_p)_0}{p_p} \right] \cdot \left[ \frac{p_s}{(p_s)_0} \right] \cdot \left[ \frac{(p_s)_0}{(p_{EX})_0} \right] \cdot (p_{EX})_0$$

considering the assumption of the analysis that

$$p_p = p_s$$

The first two pressure ratios in the above expression are simple functions of the primary and secondary Mach number, respectively, given by the relations for isentropic expansion. The third pressure ratio is the ejector pressure ratio, to be considered a constant in the optimization process. The last factor in the expression, the total exit pressure, is also a constant. Under these conditions, lines of constant supply pressure can be entered into the ejector performance diagram which uses the primary and secondary Mach number as coordinates. To enter these lines of constant primary supply pressure, the ejector pressure ratio must be given. However, the supply pressure parameter can be non-dimensionalized to make it independent of any specific ejector problem. By dividing out the constant magnitudes in the above expression, one obtains

$$\frac{(p_p)_o}{(p_s)_o} \equiv \frac{(p_p)_o}{p_p} \frac{p_s}{(p_s)_o}$$

Since  $(p_s)_o$  on the left side is a constant for a given case, the pressure ratio on the left side is a minimum whenever the primary supply pressure  $(p_p)_o$  is a minimum. For given operating media, this pressure ratio is now solely a function of the primary and secondary Mach number and can be made a generally valid part of the performance diagram. Examples in the next section will show this.



## SECTION IV

### OPTIMIZATION EXAMPLES

#### 1. ANALYTIC RESULTS

##### a. Examples for the Optimization Process

The amended optimization process has been used to calculate three examples. The results are shown in Figures 3, 4, and 5. In each case the ejector performance in terms of the ejector pressure ratio and the mass flow ratio is given. Thus, for the indicated performance, each figure gives all the ejector geometries possible within the frame of the figure. The ejector geometry at any point of the optimization plot can be read from the parameter curves for the mixing section reduction ratio  $t$  and the inlet area ratio  $A_p/A_s$ . The operating conditions are given by the primary and secondary Mach number to be read from the coordinates. The parameter  $\pi$  gives information about the type of mixing.

On their left side, the optimization plots are limited by choking conditions. The "envelope" curves on this side are therefore the choking boundaries of the plots. These envelope curves have been separately determined and entered in Figure 6. Also entered in this figure are the supply pressure ratio lines discussed in Section III 5. Where an envelope curve becomes tangent to a pressure ratio curve, optimum operating conditions are obtained since at this point the primary supply pressure becomes the lowest one possible for the given ejector performance. The optimum points I, II, and III have also been entered in the respective optimization plots in Figures 3, 4, and 5 so that the applicable ejector geometry and the operating conditions can be determined.

For instance, in Figure 3 we find that the inlet area ratio  $A_p/A_s$  should be 0.46 and the mixing section area reduction ratio  $t$  should be 0.69 to achieve the ejector performance indicated in the Figure at a minimum primary supply pressure. The associated primary Mach number is about 3.1 and the secondary Mach number is about unity. The influence of the secondary Mach number on the performance is very limited as can

be seen from Figure 2 (see also the discussion on the optimization experiments in paragraph 2b of this Section).

For the practical application of this optimization process, it is not necessary to determine the  $\pi$  lines as done in Figures 3, 4, and 5. The  $\pi$  lines are only of interest to show that the optimum points are fairly far removed from conditions of constant pressure mixing indicated by  $\pi = 0$ . In the examples shown, the pressure rise during mixing amounts to at least 30% of the total pressure rise during mixing and supersonic diffusion. For the optimization, the t-lines in Figures 3, 4, and 5 are sufficient to determine the envelope curves necessary to fix the optimum point. For this reason, only the sequence of equations for determining the t-lines is given in the Appendix. The value of  $\pi$  can be obtained as a by-product. The time required to calculate and plot one optimization diagram on a HP 9820A calculator with a HP 9862A plotter is about 1 hour. Some special features of the examples shown here, as well as experimental optimization results, are discussed in b. below.

#### b. Special Features of the Examples

For the example in Figure 3, the performance goal was taken from the dashed line in Figure 2 near the "choking" line (point I). This provided an opportunity to check the prediction given in section II that near this point the optimum performance for the given ejector geometry occurs. If this is true, the example of Figure 3 must yield the ejector geometry of Figure 2 as a result. For practical purposes, the optimum point in Figure 3 falls into the region predicted as optimum in Figure 2. The agreement with predicted conditions can be improved by choosing a point closer to the choking line in Figure 2 for fixing the performance goal. Point IV in Figure 2 proves this. Only the envelope curve in Figure 6 was determined for this point. In Section V it is shown that the region of coincidence can actually be reduced to a well-defined point.



For the optimum point in Figure 3, we find for the mixing section reduction ratio a value of about  $t = 0.69$ , close to the value assumed in Figure 2. The same is true for the inlet area ratio  $A_p/A_s$ , a consequence of the near agreement of the inlet Mach numbers.

Another example for the agreement between prediction and result of the optimization process is shown in Figures 4 and 7. In this case the performance goal was obtained from the performance characteristic in Figure 7 (point II). This characteristic differs from the one in Figure 2 by assuming helium as the secondary medium; i.e., it is for the same ejector operated with helium as the secondary medium. In this case the meeting point for the optimum line and the choking line is very clearly given. With the help of Figure 6 (curve II) we obtain again the analytically determined optimum point (also entered in Figure 4). We find close agreement between predicted (Figure 7) and calculated optimum (Figure 4) for the inlet Mach numbers and also for the mixing section reduction ratio which has in both cases a value of 0.7. By implication, as indicated before, the inlet area ratio is also very nearly the same in each case.

In the next example, the results of which are shown in Figure 5, the performance goal is the same as the one chosen for optimization in Reference 2. The purpose of this choice was to reexamine the results of this earlier effort. A discussion follows in section IV.2 below:

## 2. OPTIMIZATION EXPERIMENTS

### a. Experimental Ejector

The ejector used in the present experiments is the same as the one used for the optimization experiments described in Reference 2. Its mixing section has a taper with an outlet to inlet crosssectional area ratio  $t = 0.7$ . The examples in Figures 3 and 4 were designed to fit this existing ejector. In the first case, the Mach number 2.7 primary nozzle described in Reference 1 was used. For the second case, a new nozzle was fabricated, consisting of four single Mach number 3.2

nozzles. The subdivision into four nozzles was necessary to assure as much as possible complete mixing within the given length of the mixing section. Essential dimensions of the experimental ejector are entered in Table I.

#### b. Experimental Results

Figure 2 contains the experimental point 81E' (the designation of the point is the run number in the test records). The experimental point itself is drawn in the shape of a triangle. This triangle comes about by entering the primary and secondary Mach number as well as the parameter values resulting from the test into the characteristic; i.e., the data evaluated from the test (see Table I) for primary and secondary Mach number, as well as for mass flow ratio and ejector pressure ratio, fall into the realm of the triangle.

The size of the triangle is an indication for the accuracy of the analytic prediction for the test point. The comparatively large triangle for test point 81E' indicates poor agreement. This, however, is a necessary result since in this particular case the analytic assumptions do not properly match the test conditions. Whereas the ejector characteristic in Figure 2 was prepared under the assumption of an ideal primary nozzle, which is always properly adjusted to the operating Mach number, test point 81E' was obtained with a Mach number 2.7 nozzle instead of a Mach number 2.99 as ideally required by the characteristic. The test evaluation accounts for these off-design conditions. A check with analytic predictions considering off-design nozzle conditions (see Reference 2) revealed a quite satisfactory agreement between test and analysis. In addition the test point falls directly on the "optimum line" valid for the indicated off-design conditions. By inference it can be assumed that test run 81E' would have resulted in an essentially better agreement in Figure 2 if a primary nozzle designed close to Mach 3 were used. It is therefore justified to state that the optimization process can provide very realistic predictions.

TABLE I. EJECTOR TEST EVALUATION

| Test Run No. | Test Data                                  |                      |                      |                         |   |                             |                           |  | Test Evaluation |  |  |                   |                                      | nozzle arrangem.  |
|--------------|--|----------------------|----------------------|-------------------------|---|-----------------------------|---------------------------|--|-----------------|--|--|-------------------|--------------------------------------|-------------------|
|              | (P <sub>Ex</sub> )° =<br>barom. press. "Hg | (T <sub>p</sub> )° F | (T <sub>g</sub> )° F | (p <sub>p</sub> )° psig | sec. supply press. be-<br>fore sonic orif. psig | sonic orifice diam.<br>inch | sec. plenum vacuum<br>"Hg | Δp = (p <sub>s</sub> )° - p <sub>s</sub> "H <sub>2</sub> O | M <sub>p</sub>  | M <sub>g</sub><br>derived from Δp<br>(*) | M <sub>g</sub><br>derived from<br>M <sub>p</sub> & m <sub>p</sub> /m <sub>g</sub> (**) | $\frac{m_p}{m_g}$ | $\frac{(P_{Ex})^\circ}{(P_s)^\circ}$ |                   |
| 69B          | 29.53                                      | 58                   | 58                   | 87.2                    | 119   | 0.215                       | -19.65                    | 27   | 2.778           | 0.577                                    | 0.529  | 2.555             | 2.989                                | one M2.7 nozzle   |
| 80C          | 29.02                                      | 70                   | 60                   | 97.6                    | 29.5  | 0.315                       | -22.92                    | 25   | 3.261           | 0.743                                    | 0.819  | 3.96              | 4.757                                | one M3.2 nozzle   |
| 81E'         | 29.43                                      | 72                   | 68                   | 104                     | 60  | 0.315                       | -19.99                    | 44.6   | 2.993           | 0.808                                    | 0.868  | 2.477             | 3.118                                | one M2.7 nozzle   |
| 91'          | 29.23                                      | 70                   | 80                   | 102                     | 48  | 0.215                       | -22.9                     | 9.0  | 3.072           | 0.369                                    | 0.378  | 16.04             | 4.618                                | four M3.2 nozzles |

\*) only for comparison (not reliable, see Ref 2)

\*\*) used for plotting test points

Ejector dimensions necessary for evaluation:

primary nozzle throat diam.: 0.394"

(for tot. area for run 91')

mixing section inlet diam.: 1.50" (1.54" for 69B)

Other essential ejector dimensions:

length of mixing section: 10.5" (8" for 69B)

length of supersonic diff.: 14.2"

diverg. angle of subs. diff.: 8°



Test point 69B, also entered in Figure 2, is an example for good agreement between experiment and analytic prediction. In this case, the test point has been obtained with a Mach number very close to the design Mach number of the primary nozzle. This is also true for test point 80C discussed next.

Figure 2 contains also a rerun (point 80C) of the "optimum" point given in Reference 2. We see that the point is close to the line of optimum conditions, but removed from the predicted absolute optimum. The apparent reason is that the geometry of the present experimental ejector is not optimum for the chosen performance. Figure 5 provides the geometry for optimum conditions in this case. We see as a result that the primary Mach number can be lowered from about 3.25 to 3. However, the mixing section taper would have to be reduced from 0.7 to about 0.6 to obtain this reduction in primary Mach number.

The experiments with helium as the secondary operating medium encountered difficulties in reaching the optimum performance point. Test point 91' entered in Figure 7 came closest to the optimum performance point in this figure. While the predicted optimum was for a pressure ratio 5 and a mass flow ratio of 14, the corresponding numbers for the best experimental performance were 4.6 and 16. This experimental performance, however, was well within analytic predictions. Near the optimum performance point it is typical that small performance changes require large changes in flow conditions. In the experiment with helium the primary Mach number would have required an increase from 3.1 to 3.4 and the secondary Mach number from 0.38 to 0.8 to reach optimum performance. Apparently these necessary flow changes come in conflict with mixing requirements, spoiling the performance near the optimum point.

An essential portion of the discrepancy between analysis and experiment can be traced to a kind of flow instability in the air-helium mixing process. This conclusion is based on the following experimental observations. In these tests helium was admitted to the ejector only for the time when measurements were actually taken. Outside these

periods, air was admitted at the same secondary supply pressure as that of the helium. A solenoid valve system provided a fast switchover from air to helium. At the time of switchover to helium, the ejector pressure ratio dropped off in a staggering fashion, taking nearly 1 second to arrive at a steady performance level. According to predictions, there should have been only a very small drop in pressure ratio for helium operation. Since the time of performance deterioration was much longer than the switchover time, the required performance for helium apparently existed momentarily after switchover. Apparently instabilities in the mixing process are responsible for the deterioration. The point for this momentary performance is also entered in Figure 7, marked as square. This new point is much closer to the perfect optimum. It can serve as an indication that the optimization process is, in principle, correct also for helium operation. However, mixing problems prevent the realization of analytically predicted conditions in steady-state operation.



## SECTION V

## EJECTOR OPERATION IN TERMS OF THE FLOW DENSITY PARAMETER

## 1. THE FLOW DENSITY PARAMETER

The "flow density parameter" is a dimensionless magnitude which appears in the process of solving the ejector equations (see Reference 1). It has some unique features which make it suitable for characterizing the flow conditions in an ejector. A graphic presentation of this parameter as a function of the mixing section exit Mach number provides a particularly useful tool for studying ejector operations.

The nature of this parameter is best understood by discussing Equation 21c of Reference 1, from which it originated. For convenience, this equation is repeated here:

$$\frac{M_{Ex-m} \left( 1 + \frac{\gamma_{Ex-1}}{2} M_{Ex-m}^2 \right)^{\frac{1}{2}}}{\gamma_{Ex} M_{Ex-m}^2 c_m \tau} = E = \frac{M_s \left( \frac{m_p}{m_s} + 1 \right)}{B_m t \left( \frac{A_p}{A_s} + 1 \right)} \sqrt{\frac{\left( 1 + \frac{m_p R_p}{m_s R_s} \right) \left( \frac{c_{p-p} m_p (T_p)_0}{c_{p-s} m_s (T_s)_0} + 1 \right) (T_s)_0}{\left( 1 + \frac{m_p \gamma_p}{m_s \gamma_s} \right) \left( \frac{c_{p-p} m_p}{c_{p-s} m_s} + 1 \right) T_s}} \quad (21c) \text{ Ref 1}$$

The magnitude, which both sides represent, is the flow density parameter (E) (some notations of Reference 1 have been slightly changed here). The left side of the equation is a function of the mixing section exit conditions; the right side of the equation is a function of the mixing section inlet conditions. Mixing section wall friction is included in the exit conditions by the factor  $c$  (for this factor see Equations 2 and 3 in the Appendix). Wall pressure forces, which appear in a tapered mixing section due to pressure differences along the mixing section, are also accounted for. These forces are a function of the taper of the mixing section, the pressure difference between inlet and exit, and the shape of the pressure distribution curve along the mixing section. The taper and the shape of the pressure distribution curve enter the flow density parameter in the form of the magnitude  $\tau$ , defined according to Equation 41 of Reference 1 as

$$\tau = \frac{i}{2} \left( \frac{1}{t} - 1 \right) + 1 \quad (41) \text{ Ref 1}$$

The magnitude  $\tau$  enters only the left side of Equation 21c and can be considered constant for a given ejector problem. The taper of the mixing section, which enters the right side of Equation 21c and is given with the geometry of the ejector, is truly a constant. The character of the pressure distribution is not an inherent constant. However, as mentioned before, it changes only slightly with the ejector operating conditions and may be considered a constant as a reasonable approximation.

The meaning of Equation 21c for the ejector analysis is the following:  
 a) The right side allows an E value to be determined from ejector geometry and inlet flow conditions. b) With this E value, the left side can be solved for the mixing section exit Mach number (Equation 22c, Ref 1). Equation 21c is derived on the basis of conservation of mass, momentum, and energy in the presence of wall effects. The flow density parameter is a constant of the mixing process, from which the exit flow conditions can be derived as a function of the wall effects.

As shown in the Appendix, Equation 43, the flow density parameter can be expressed as the ratio of the exit mass flow density over the inlet momentum flow density made dimensionless by the stagnation speed of sound of the mixed media. Since the latter magnitude is independent of the details of the mixing process, it remains constant as long as the inlet conditions are not changed. Also, at a given exit geometry the exit flow density in this ratio cannot be changed unless the inlet conditions are changed. Thus the ratio is a function of the inlet conditions only. This confirms the property of E as represented by the right side of Equation 21c which contains, besides geometric conditions, only magnitudes given at the inlet. The presence of supersonic shocks or wall friction changes the exit Mach number but not E.

## 2. THE FLOW DENSITY PLOT

The practical application of the flow density parameter will be shown with an example. We take the ejector performance curve for pressure ratio of 4 in Figure 8 as example to study the flow conditions involved (the characteristic in Figure 8 is taken from Figure 2.) For this study we use a graphic presentation of  $E$  as given by the relation of the left side of Equation 21c. Using the mixing section taper and the wall friction data, which apply to the performance characteristic in Figure 8, we arrive at the plot given in Figure 9. Altogether three curves result. The solid line is for the actual mixing section. The two dashed curves are for the supersonic diffuser, which is treated as an ejector (see Section III 3). The upper dashed curve is for zero wall friction and the lower dashed curve is for the diffuser with wall friction as indicated in Figure 2.

We need the curve for zero wall friction to determine the flow density parameter of the supersonic diffuser. For zero wall friction and a constant crosssectional area of the duct, the inlet and exit Mach number of the duct are the same in the absence of supersonic shocks. Thus the top curve in Figure 9 applies also for the inlet Mach number. If the inlet Mach number, (subsonic or supersonic) is known, the flow density parameter can be determined from the plot. The exit Mach number for flow conditions with supersonic shocks and with wall friction can then be determined. If, for example, the inlet Mach number is 2, the  $E$  value we read from the top curve is 0.41. Moving in Figure 9 along this value to the first intersection with the lower dashed curve yields the exit Mach number for the case that no shocks occur. The decrease in Mach number is then due only to the presence of wall friction. If we move to the second intersection, which is in the subsonic region, we obtain the exit Mach number after shock diffusion in the presence of wall friction. If we move further on to the intersection with the top curve, again we obtain the subsonic exit Mach number, without wall friction. In general a given  $E$  value has two possible exit Mach numbers, a subsonic and a supersonic one. However, the top point of each curve does not coincide with Mach number 1 at the abscissa, except for the uppermost curve for which the wall effects are zero.



The plot also contains curves of constant pressure made dimensionless by the inlet momentum flow density (see Appendix). These constant pressure lines are independent of wall friction. The momentum flow density, however, is a function of  $\tau$  and the inlet flow conditions. For a given case of ejector operation; i.e., for a given  $E$ , the momentum flow density is a constant. Therefore the ratio between two pressure values read from the curves, for two points with the same  $E$ , gives the pressure ratio between these two points. For instance, in the simple case of a constant area duct with no wall friction (upper dashed curve) a line of constant  $E$  yields the static pressure ratio across a normal shock for the supersonic Mach number marked by the intersection of the  $E$  line with the top curve.

### 3. TYPICAL OPERATING CONDITIONS

In carrying through our example we mark three points (a-c) on the performance curve selected in Figure 8. The associated  $E$  values found from the analysis are marked in Figure 9. These points should not be visualized as a sequence of flow conditions occurring in an experimental run; but rather, each point can serve as a case for explaining a typical set of flow conditions.

#### a. Conditions for Supersonic Mixing

If we consider point a in Figure 9 we find that the density parameter allows a supersonic solution with an exit Mach number of about 3. This exit Mach number is much higher than the primary Mach number. To produce this high exit Mach number, a flow acceleration would have to take place during mixing. Since we have a mixing section with decreasing crosssection, acceleration is not possible after mixing. Acceleration, however, is possible prior to mixing. Upon entering the mixing section, the already supersonic primary flow can expand to increase its Mach number. At the same time, the subsonic secondary flow can increase its Mach number in the space left between the expanding primary flow and the mixing section wall. Since the mixing process is a dissipative process, the fully expanded primary Mach number must always be higher than the exit Mach number.



Though flow expansion in the mixing section is possible it cannot be realized unless the ejector is able to provide the necessary pressure drop. In the present case, the ejector is obviously not able to provide the pressure ratio necessary to produce the exit Mach number required to satisfy the supersonic solution. Thus only the subsonic solution is possible. For subsonic mixing, the pressure always rises during mixing and no expansion occurs in the mixing section. A transition from subsonic to supersonic mixing can only occur if it does not require a pressure drop in the mixing section. This is possible if the resulting supersonic exit Mach number is sufficiently below the primary Mach number. There is a well-defined condition where given inlet conditions allow a supersonic exit Mach number without a pressure drop. This is the condition of constant pressure mixing. The point where this condition is fulfilled can be identified in Figure 9. Considering Equation 44 in the Appendix, the pressure ratio in this equation becomes unity for constant pressure mixing. Thus the pressure parameter  $P$  in Figure 9 becomes equal to the inverse of the magnitude  $B$  which is given by the inlet condition according to Equation 9e of Ref 1:

$$B = \frac{\gamma_p M_p^2}{t \left(1 + \frac{A_s}{A_p}\right)} + \frac{\gamma_s M_s^2}{t \left(1 + \frac{A_p}{A_s}\right)} + \tilde{\tau} \quad (9e) \text{ Ref 1}$$

For point a, we find that  $1/B$  is much larger than the  $P$  value we read for the supersonic solution in Figure 9, indicating that a pressure drop during mixing would be required to produce a supersonic exit Mach number.

#### b. Mixing Mode Transition

Point b fulfills the condition for constant pressure mixing, which allows transition to supersonic mixing. At the point of the supersonic solution, we read for the dimensionless pressure a value of 0.153. This value is equal to  $1/B$ . The point of constant pressure mixing can also be predetermined from Figure 8. It occurs along the line  $\pi = 0$  drawn into Figure 8. In reality only the performance above

this line is possible. Below this line the subsonic solution applies, which gives a performance inferior to the one shown in Figure 8 for the supersonic solution.

For the mixing mode transition at point b, it is essential to consider the stability of the flow created by the transition. In changing from subsonic to supersonic mixing, a drastic change in the pressure distribution in the mixing section occurs, resulting in greatly improved ejector performance. This can be seen for point b in Figure 9 if one reads the dimensionless pressure  $P$  at the point of the supersonic diffuser exit in each case. For the subsonic case (solid circle), we read a value of 0.52, while for the supersonic case (open circle), the value is 0.62. To account for the difference in inlet momentum for the supersonic diffuser in each case, the ratio of the unitized pressures must be multiplied with the ratio of the respective  $E$  values. Accomplishing this one obtains a pressure ratio of 1.28; i.e., the pressure at the supersonic diffuser exit is 28% higher in the supersonic mixing case. Considering the lesser subsonic pressure recovery in the supersonic mixing case, a net increase of 14% remains. This increase in performance comes about when the transition occurs. An initial increase of the ejector pressure ratio allows an increase in primary and secondary Mach numbers, a process which improves the ejector performance. Thus the increase in performance continues until either a balance between increased pressure ratio and increased primary Mach number is reached or the ejector geometry limits any further expansion. For the present example it can be shown that a considerable overexpansion in the mixing section inlet takes place. Above point b in Figure 8 the constant pressure ratio lines run almost parallel with the constant mass ratio lines. A slight increase in pressure ratio allows the operating point to move along a constant mass ratio line to higher primary and secondary Mach numbers. Since the ejector geometry does not allow any further expansion if both media are supersonic, a Mach number of 1 constitutes a kind of limit for the secondary Mach number.

Not everywhere in the characteristic shown in Figure 8 are the pressure ratio and mass ratio curves nearly parallel at the point of transition. For instance, at very high pressure ratios the curves cross at a large angle at the transition point. For the operating point to move along a constant mass ratio line, a comparatively large change in pressure ratio is necessary. The consequence is that the operating point, where the flow stabilizes itself after the transition, will not be far from the transition point (see Figure 4 of Reference 2).

The endstate of transition can no longer be truly identified in Figure 8 since, as we will see in the next section, a change in the wall friction conditions for the supersonic diffuser occurs as consequence of the transition. If we assume that the increase of the inlet Mach numbers occurs in a free expansion outside the primary nozzle, no new forces enter the flow system of the mixing section and the flow density parameter must stay constant during transition.

#### c. The Limiting Mach Number

In the mixing mode transition process the primary Mach number can only increase to a certain value fixed by the ejector geometry. This limiting condition has an essential influence on the ejector operation. An increase in primary flow cannot change this limiting Mach number, and the ejector pressure ratio cannot increase at a given secondary flow rate. Thus with the mixing section Mach numbers fixed, any change in ejector flow rate increases or decreases only the pressure in the mixing section. This change in pressure has the effect of moving the supersonic shock system in the ejector upstream or downstream. If the primary flow is increased, the shock system moves downstream. The consequence is that more wall area is exposed to supersonic flow conditions, and the performance drops. If the pressure is decreased, the reverse happens.



The limit for the upstream movement of the shock system in the supersonic diffuser is reached at the exit of the mixing section. This is the condition for the best performance at a given secondary flow rate, since a minimum of wall area is exposed to supersonic flow conditions. If the ejector flow rate is further reduced, the shock system enters the mixing section, spoiling the pressure distribution in the mixing section. This causes the mixing mode to change back to subsonic, with a sudden collapse in performance. The resulting subsonic operating point is always at a lower ejector flow rate than that required for transition to the supersonic mode.

This hysteresis in the mode transition can be explained in the following way. In the process of transition the limiting Mach number is generally reached before the increase in ejector pressure ratio, due to the transition, is completely utilized. The resulting "excess" of pressure in the mixing section pushes the supersonic shock system downstream until a balance between increased wall friction and excess pressure is reached. This phenomenon is a typical experimental experience (For example, see Figure 11 of Reference 2). To reverse the transition process, the primary flow has to be reduced until the shock system is moved back to the mixing section exit. Only then does a further primary flow reduction reverse the transition, which results in performance collapse.

In the case of a constant area mixing duct, the wall pressure forces are zero in the direction of flow, and no performance change occurs during the mode transition; consequently, no hysteresis appears in this case.

#### 4. OPTIMUM PERFORMANCE

In our example, the "optimum performance" is reached at point c, where the pressure ratio line becomes tangent to the mass flow ratio line in Figure 8; i.e., the mass flow ratio becomes a minimum. At this point the flow density parameter becomes a maximum for the chosen pressure ratio curve in Figure 8. It has, however, not reached its highest possible value. This top value is given by the base line of the shaded area in Figure 9. For the E value at this line, the supersonic diffuser exit



becomes choked, as one can see by continuing the process to the dashed lines in Figure 9.

Since the E curves in Figure 9 are valid for any point in the characteristic of Figure 8, we may survey the characteristic for trends to increase E to eventually obtain the highest possible value. By moving from point c in Figure 8 to the right along the optimum line we find that E decreases. For instance, at the pressure ratio 6 on this line, E has dropped to a value of 0.375 compared to 0.394 at point c. If we move on the dashed line to the left of point c, the flow density parameter increases to reach, at the end of the line, its highest possible value which is, in our case, 0.409. Thus we have reached the point of the absolute optimum in Figure 8.

If we would be able to decrease the wall friction in the supersonic diffuser, the shaded area would become smaller; i.e., a higher E value would be possible. This would also move the choking line more to the left in Figure 8. With a further decrease in wall friction, the shaded area disappears and the top value of the solid curve, i.e., the mixing section, itself determines the highest possible flow density. A similar effect is obtained if the wall friction of the mixing section is increased. This lowers the solid curve, making the shaded area (the influence of the supersonic diffuser) disappear. Thus choking can have different causes.

If, in returning to our example, we move along the choking line in Figure 8, we find that E remains constant, i.e., at its highest possible value. This, however, does not mean that all performances along this line are absolute optima. For instance, if we take in Figure 8, point V on this line and determine the optimum envelope curve for the performance at this point, we find that point V, as shown in Figure 6, falls on this curve (open circle); however, it is removed from the absolute optimum (solid circle) where the supply pressure ratio is the lowest. If we check the ejector geometry for this optimum point, we find that the improvement was obtained by increasing the mixing section reduction ratio from 0.7 to 0.73, i.e., decreasing the taper.

If we would introduce this new taper in our example in Figure 9, the solid curve would move upward causing the base-line of the shaded area to move to a larger  $E$ . For the inlet conditions of point  $c$ , the flow density parameter would drop with the new taper. This implies that the previous performance could not even be maintained at this inlet condition. The only performance which can utilize the increased  $E$  value is the one belonging to point  $V$  in Figure 8, as demonstrated by the optimum envelope curve for this performance. In the optimization process, the performance is given. In terms of the flow density parameter, optimization means finding the mixing section taper which gives  $E$  the highest value possible for the desired performance.

## SECTION VI

## CONCLUSION

The optimization of an ejector, i.e., finding the ejector geometry which produces a given performance with a minimum of primary supply pressure, can be readily solved analytically, accounting also for wall and diffusion losses. (The sequence of equations for carrying out an optimization process is given in the Appendix). Experiments with air as operating media confirm the analytic results. In case of helium as secondary medium, it was not quite possible to reach the predicted optimum performance. Mixing difficulties enhanced by the flow conditions peculiar to optimum performance were the apparent cause for the discrepancies.

A dimensionless magnitude, which appears in the process of solving the ejector equations and which has been termed "flow density parameter" since it can be interpreted as the ratio of mass flow density over momentum flow density made dimensionless by the stagnation speed of sound, proved to be useful for a graphic interpretation of ejector operations.

With the help of a diagram, in which this parameter is plotted as a function of the exit Mach number of the mixing section as well as the supersonic diffuser, operational states essential for the understanding of the ejector mechanism can be identified. One such state is where supersonic mixing, i.e., mixing with a supersonic exit Mach number, becomes admissible. Another such state is where the actual transition from subsonic to supersonic mixing occurs in a real ejector. This transition is a general prerequisite for achieving optimum operating conditions in an ejector. Physically it occurs where constant pressure mixing has been reached. The plot of the flow density parameter gives a particularly clear picture of the conditions where choking in the ejector occurs and shows that optimization of an ejector means maximizing the flow density parameter.

## APPENDIX

## CALCULATOR PROGRAMS AND DERIVATIONS

Numbers on the left side of equations refer to equations of Ref 1 (or Ref 2 if so indicated) with which the listed equation is identical or from which it is derived. Equations without identification on the left side are either well-known thermodynamic relations or simple substitutions.

1. EQUATIONS FOR CALCULATING AN EJECTOR PERFORMANCE CHARACTERISTIC (FIG 2 or 7)

Input Data:

$\gamma_p$

$\gamma_s$

$R_s/R_p$

$(T_p)_\infty / (T_s)_\infty$

$\eta_{pol}$

$[c_f L / (2D)]_m$  referred to  $M_{ex-m}$

$[c_f L / (2D)]_d$  referred to  $M_{ex-d}$

$i = 0.8$  for supersonic mixing

$\left. \begin{matrix} t \\ (A_p/A_s)_{Ref} \\ M_{Ref} \end{matrix} \right\} \text{reference layout of ejector *)}$

- \*) Under the assumption of a fixed crosssectional inlet area and taper of the mixing section, Eqs 20 and 21 of the sequence of equations below calculate a new  $A_p/A_s$  for any other primary Mach number  $M_p$  occurring in the characteristics of Figs 2 or 7, i.e., the primary nozzle is always correctly expanded for any point in these characteristics.



## a. Pressure Ratio Curves

Select parameter value:  $(p_{Ex})_o / (p_s)_o$ Independent variable:  $M_s$ 

The equations are solved by iteration of  $f$  and  $A_p/A_s$  (Eqs 18 and 21 below). As a first approximation assume

$$f = 1.4$$

$$A_p/A_s = (A_p/A_s)_{Ref}$$

start with  $(p_{Ex})_o / (p_s)_o$  as close to reference conditions as possible.

Sequence of equations for calculator program:

$$\frac{C_{p-s}}{C_{p-p}} = \frac{R_s}{R_p} \cdot \frac{\gamma_s}{\gamma_p} \cdot \frac{(\gamma_p - 1)}{(\gamma_s - 1)} \quad (1)$$

$$C_m = 1 + \left[ \frac{C_f L}{2D} \right]_m \quad (2)$$

$$C_d = 1 + \left[ \frac{C_f L}{2D} \right]_d \quad (3)$$

$$41 \quad \tilde{t} = 1 + \frac{1}{2} \left( \frac{1}{t} - 1 \right) \quad (4)$$

$$\frac{(T_s)_o}{T_s} = 1 + \frac{\gamma_s - 1}{2} M_s^2 \quad (5)$$

$$\frac{(p_s)_o}{p_s} = \left[ \frac{(T_s)_o}{T_s} \right]^{\frac{\gamma_s}{\gamma_s - 1}} \quad (6)$$

$$57 \quad B_m = \frac{(p_{Ex})_o}{(p_s)_o} \cdot \frac{(p_s)_o}{p_s} \cdot f \quad (7)$$

$$9e \quad M_p = \sqrt{\frac{t(1+\frac{A_s}{A_p})}{\gamma_p} \cdot B_m - \frac{\gamma_s M_s^2}{\gamma_p \frac{A_p}{A_s}} - \tau \cdot t \frac{(1+\frac{A_s}{A_p})}{\gamma_p}} \quad (8)$$

$$5 \quad \frac{m_p}{m_s} = \sqrt{\frac{A_p^2 \gamma_p R_s (T_s)_0 M_p^2 [2 + (\gamma_p - 1) M_p^2]}{A_s^2 \gamma_s R_p (T_p)_0 M_s^2 [2 + (\gamma_s - 1) M_s^2]}} \quad (9)$$

$$16 \quad \gamma_{Ex} = \left(1 + \frac{m_p}{m_s} \frac{\gamma_p}{\gamma_s}\right) \quad (10)$$

$$21c \quad E_m = \frac{M_s(1+\frac{m_p}{m_s})}{B_m t(1+\frac{A_p}{A_s})} \sqrt{\frac{(1+\frac{m_p}{m_s} \frac{R_p}{R_s})(\frac{C_{p-p}}{C_{p-s}} \frac{m_p}{m_s} \frac{(T_p)_0}{(T_s)_0} + 1)(T_s)_0}{(1+\frac{m_p}{m_s} \frac{\gamma_p}{\gamma_s})(\frac{C_{p-p}}{C_{p-s}} \frac{m_p}{m_s} + 1) T_s}} \quad (11)$$

$$\alpha_m = 2 \gamma_{Ex} E_m^2 c_m \quad (12)$$

$$22c \quad M_{Ex-m}^2 = \frac{1 - \left[ -\sqrt{1 - \frac{\alpha_m \tau^2}{c_m} \left( 2 \frac{c_m}{\tau} + \frac{1}{\gamma_{Ex}} - 1 \right) + \alpha_m \tau} \right]}{c_m \alpha_m \gamma_{Ex} - \gamma_{Ex} + 1} \quad (13)$$

For the subsonic solution delete the minus sign before the root.

$$9e \quad B_d = \gamma_{Ex} M_{Ex-m}^2 + 1 \quad (14)$$

$$21c \quad E_d = \frac{M_{Ex-m}}{B_d} \sqrt{1 + \frac{\gamma_{Ex} - 1}{2} M_{Ex-m}^2} \quad (15)$$

$$\alpha_d = 2 \gamma_{Ex} E_d^2 c_d \quad (16)$$

22c 
$$M_{Ex-d}^2 = \frac{1 - \left[ \sqrt{1 - \frac{\alpha_d}{C_d} \left( 2C_d + \frac{1}{\gamma_{Ex}} - 1 \right)} + \alpha_d \right]}{C_d \alpha_d \gamma_{Ex} - \gamma_{Ex} + 1} \quad (17)$$

57 
$$f_{n+1} = \frac{(\gamma_{Ex} M_{Ex-d}^2 C_d + 1)(\gamma_{Ex} M_{Ex-m}^2 C_m + \tau)}{B_d \left[ 1 + \frac{\gamma_{Ex} - 1}{2} M_{Ex-d}^2 \right] \frac{\eta_{pol} \gamma_{Ex}}{\gamma_{Ex} - 1}} \quad (18)$$

$$[f_{n+1}]_{it} = (2f_n + f_{n+1}) \cdot \frac{1}{3} \quad (19)$$

$$\frac{A_{Ref}}{A_p} = \frac{M_p}{M_{Ref}} \left[ \frac{1 + \frac{\gamma_p - 1}{2} M_{Ref}^2}{1 + \frac{\gamma_p - 1}{2} M_p^2} \right] \frac{\gamma_p + 1}{2(\gamma_p - 1)} \quad (20)$$

25 Ref 2 
$$\frac{A_p}{A_s} = \frac{1}{\frac{A_{Ref}}{A_p} \left[ 1 + \left( \frac{A_s}{A_p} \right)_{Ref} \right] - 1} \quad (21)$$

$$\left[ \left( \frac{A_p}{A_s} \right)_{n+1} \right]_{it} = \left[ 2 \left( \frac{A_p}{A_s} \right)_n + \left( \frac{A_p}{A_s} \right)_{n+1} \right] \cdot \frac{1}{3} \quad (19a)$$

Principle result:  $M_p$

Other results:

9e 
$$\frac{P_{Ex-m}}{P_s} = \frac{B_m}{\gamma_{Ex} M_{Ex-m}^2 C_m + \tau} \quad (22) \quad \frac{P_{Ex-d}}{P_{Ex-m}} = \frac{\gamma_{Ex} M_{Ex-m}^2 + 1}{\gamma_{Ex} M_{Ex-d}^2 C_d + 1} \quad (22a)$$

use Eqs 22 and 22a to calculate  $\pi$  (see Sect III 4)

b. Mass Ratio Curves

Use Eqs 36a and 36b below with  $m_p/m_s$  as parameter.  
Determine  $A_p/A_s$  from Eqs 20 and 21 above.

2. EQUATIONS FOR PLOTTING AN OPTIMIZATION DIAGRAM (Figs 3, 4, or 5)

Input Data:

$\gamma_p$

$\gamma_s$

$R_s/R_p$

$(T_p)_o/(T_s)_o$

$\eta_{pol}$

$[c_f L/(2D)]_m$  referred to  $M_{Ex-m}$

$[c_f L/(2D)]_d$  referred to  $M_{Ex-d}$

$i = 0.8$  for supers.  $M_{Ex-d}$

a. t-Curves

Select: ejector performance  $(P_{Ex})_o/(p_s)_o$  and  $m_p/m_s$   
parameter value  $t$

Independent variable  $M_s$

The equations are solved by iteration of  $f$  (Eq 35 below). As a first approximation assume

$$f = 1.4$$

Sequence of equations for calculator program (equations which occurred already in the preceding program are only listed by their numbers):

$$\frac{C_{p-s}}{C_{p-p}} = \quad (1)$$

$$C_m = \quad (2)$$



$$C_\alpha = \quad (3)$$

$$(T_s)_0/T_s = \quad (5)$$

$$(P_s)_0/P_s = \quad (6)$$

$$\gamma_{EX} = \quad (10)$$

$$110 \quad b = \frac{\gamma_s}{\gamma_p} M_s^2 \quad (23)$$

$$111 \quad C = \frac{\gamma_p \frac{R_s}{R_p}}{\left(\frac{m_p}{m_s} M_s\right)^2 \gamma_s \frac{(T_p)_0}{(T_s)_0} [2 + (\gamma_s - 1) M_s^2]} \quad (24)$$

$$21c \quad Q = M_s \left(1 + \frac{m_p}{m_s}\right) \sqrt{\frac{\left(1 + \frac{m_p}{m_s} \frac{R_p}{R_s}\right) \left(\frac{c_{p-p} m_p (T_p)_0}{c_{p-s} m_s (T_s)_0} + 1\right) (T_s)_0}{\left(1 + \frac{m_p}{m_s} \frac{\gamma_p}{\gamma_s}\right) \left(\frac{c_{p-p} m_p}{c_{p-s} m_s} + 1\right) T_s}} \quad (25)$$

$$\tau = (4)$$

$$108a \quad \alpha_1 = \frac{t (P_{EX})_0 (P_s)_0}{\gamma_p (P_s)_0 P_s} \quad (26)$$

$$109a \quad \alpha_2 = \frac{t \cdot \tau}{\gamma_p} \quad (27)$$

$$107 \quad \alpha = \alpha_1 \cdot f - \alpha_2 \quad (28)$$

$$113 \quad A = 1 - c(\alpha - b)^2 (\gamma_p - 1) \quad (29)$$

$$114 \quad B = 2c(\alpha - b) [(\gamma_p - 1)\alpha + 1] \quad (30)$$

$$115 \quad C = c \cdot \alpha [2 + \alpha(\gamma_p - 1)] \quad (31)$$

$$116 \quad \frac{A_s}{A_p} = \frac{B + \sqrt{B^2 + 4AC}}{2A} \quad (32)$$

$$21c \quad E_m = \frac{Q}{a_1 \cdot \gamma_p \cdot f \left(1 + \frac{A_p}{A_s}\right)} \quad (33)$$

$$\alpha_m = \quad (12)$$

$$M_{EX-m}^2 = \quad (13)$$

$$B_d = \quad (14)$$

$$E_d = \quad (15)$$

$$\alpha_d = \quad (16)$$

$$M_{EX-d}^2 = \quad (17)$$

$$9e \quad \frac{P_{EX-d}}{P_{EX-m}} = \frac{\gamma_{EX} M_{EX-m}^2 + 1}{\gamma_{EX} M_{EX-d}^2 C_d + 1} \quad (34)$$

$$47 \quad f = \frac{\gamma_{EX} M_{EX-m} C_m + \tilde{C}}{\frac{P_{EX-d}}{P_{EX-m}} \left[ 1 + \frac{\gamma_{EX} - 1}{2} M_{EX-d}^2 \right] \frac{\eta_{pol} \gamma_{EX}}{\gamma_{EX} - 1}} \quad (35)$$

$$105a \quad M_p^2 = \left(1 + \frac{A_s}{A_p}\right) \alpha - \frac{A_s}{A_p} b \quad (36)$$

Principle result:  $M_p$  and  $A_p/A_s$

## b. Envelope Curve

The points for which the root either in Equation 13 or 17 becomes zero (choking condition) establish the "envelope curve" necessary to find the optimum ejector layout as shown in Figure 6. The iteration process in the present calculations begins to fail near the zero root conditions. This failure, which results in a negative root, is for practical purposes a sufficient criterion to mark points for the envelope curve.

c.  $(A_p/A_s)$  Curves

For plotting the  $(A_p/A_s)$ -curves Equation 9 is either solved for the primary or secondary Mach number. If we choose the secondary Mach number for the solution the result is:

$$44 \quad M_s^2 = \frac{\sqrt{1 + N(\gamma_s - 1)} - 1}{(\gamma_s - 1)} \quad (36a)$$

where

$$45 \quad N = \left[ \frac{A_p}{A_s} \frac{m_s}{m_p} \right]^2 \frac{\gamma_p R_s (T_s)_0}{\gamma_s R_p (T_p)_0} M_p^2 \left[ 2 + (\gamma_p - 1) M_p^2 \right] \quad (36b)$$

$M_s$  can then be plotted against  $M_p$  as independent variable with  $A_p/A_s$  as a parameter.

## 3. INTERPRETATION OF THE FLOW DENSITY PARAMETER

The following interpretation consists only in substitutions by well known thermodynamic relations.

$$21c \quad E = \frac{M_{EX} \left( 1 + \frac{\gamma_{EX} - 1}{2} M_{EX}^2 \right)^{\frac{1}{2}}}{\gamma_{EX} M_{EX}^2 C + \tau} \quad (37)$$

$$= \frac{V_{EX} \sqrt{(T_{EX})_0 / T_{EX}}}{\sqrt{R_{EX} T_{EX} \gamma_{EX}} (\gamma_{EX} M_{EX}^2 C + \tau)} \quad (38)$$

$$= \frac{V_{EX} \sqrt{(T_{EX})_0}}{\sqrt{R_{EX} \gamma_{EX}} T_{EX} (\gamma_{EX} M_{EX}^2 C + \tau)} \times \frac{\sqrt{(T_{EX})_0} R_{EX} p_{EX} (p_{EX})_0}{\sqrt{(T_{EX})_0} R_{EX} p_{EX} (p_{EX})_0} \quad (39)$$

$$= \frac{V_{EX} (T_{EX})_0 R_{EX} p_{EX} (p_{EX})_0}{\sqrt{R_{EX} \gamma_{EX} (T_{EX})_0} (p_{EX})_0 T_{EX} R_{EX} (p_{EX} \gamma_{EX} M_{EX}^2 C + p_{EX} \tau)} \quad (40)$$

$$= \frac{V_{EX} p_{EX} (p_{EX})_0}{a_0 (p_{EX})_0 (p_{EX} \gamma_{EX} M_{EX}^2 C + p_{EX} \tau)} \quad (41)$$

$$= \frac{\frac{V_{EX} p_{EX}}{a_0 (p_{EX})_0}}{\frac{V_{EX}^2 p_{EX} C + p_{EX} \tau}{(p_{EX})_0}} \quad (42)$$

$$= \frac{\text{dimensionless exit mass flow density}}{\text{dimensionless inlet momentum flow density}}$$

The inlet momentum flow density is expressed in terms of the exit conditions with the help of friction factor  $c$  and wall force factor  $\tau$ . Equation 42 can be also transformed into

$$E = \frac{V_{EX} p_{EX}}{(V_{EX}^2 p_{EX} C + p_{EX} \tau)} \cdot \frac{a_0}{\gamma_{EX}} \quad (43)$$



## 4. INTRODUCTION OF A PRESSURE PARAMETER IN FIG 9

$$21c \quad E = \frac{M_{EX} \left( 1 + \frac{\gamma_{EX}-1}{2} M_{EX}^2 \right)^{\frac{1}{2}}}{\gamma_{EX} M_{EX}^2 C + \tau}$$

$$9e \quad B = \frac{P_{EX}}{P_S} (\gamma_{EX} M_{EX}^2 C + \tau)$$

$$E = M_{EX} \left( 1 + \frac{\gamma_{EX}-1}{2} M_{EX}^2 \right)^{\frac{1}{2}} \cdot \frac{P_{EX}}{(P_S B)} \quad (44)$$

Eq. 44 is plotted in Fig 9 with

$$\frac{P_{EX}}{(P_S B)} = p$$

as parameter. The unitizing expression  $(p_s B)$  is the inlet impuls density and can be expressed by the mixing section inlet conditions:

$$9e \quad (P_S B)_m = P_S \left[ \frac{\gamma_P M_P^2}{t \left( 1 + \frac{A_S}{A_P} \right)} + \frac{\gamma_S M_S^2}{t \left( 1 + \frac{A_P}{A_S} \right)} + \tau \right] \quad (45)$$

or in case of a constant area supersonic diffuser

$$(P_S B)_d = P_S \left[ \gamma_{EX} M_{EX-m}^2 + 1 \right] \quad (46)$$

REFERENCES

1. Hasinger, S., "Performance Characteristics of Ejector Devices," Aerospace Research Laboratories, Technical Report ARL TR-75-0205, Wright-Patterson AFB, Ohio, June 1975.
2. Hasinger, S. and Fretter E., "Comparison of Experiment and Analysis for a High Primary Mach Number Ejector," Air Force Flight Dynamics Laboratory, Technical Report AFFDL-TR-77-38, Wright-Patterson AFB, Ohio, May 1977.

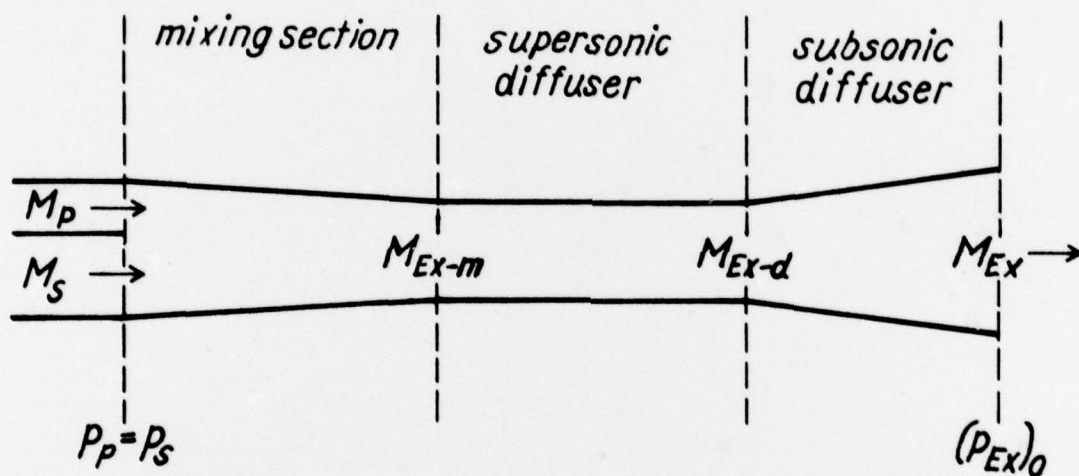


Figure 1. Ejector Flow Scheme

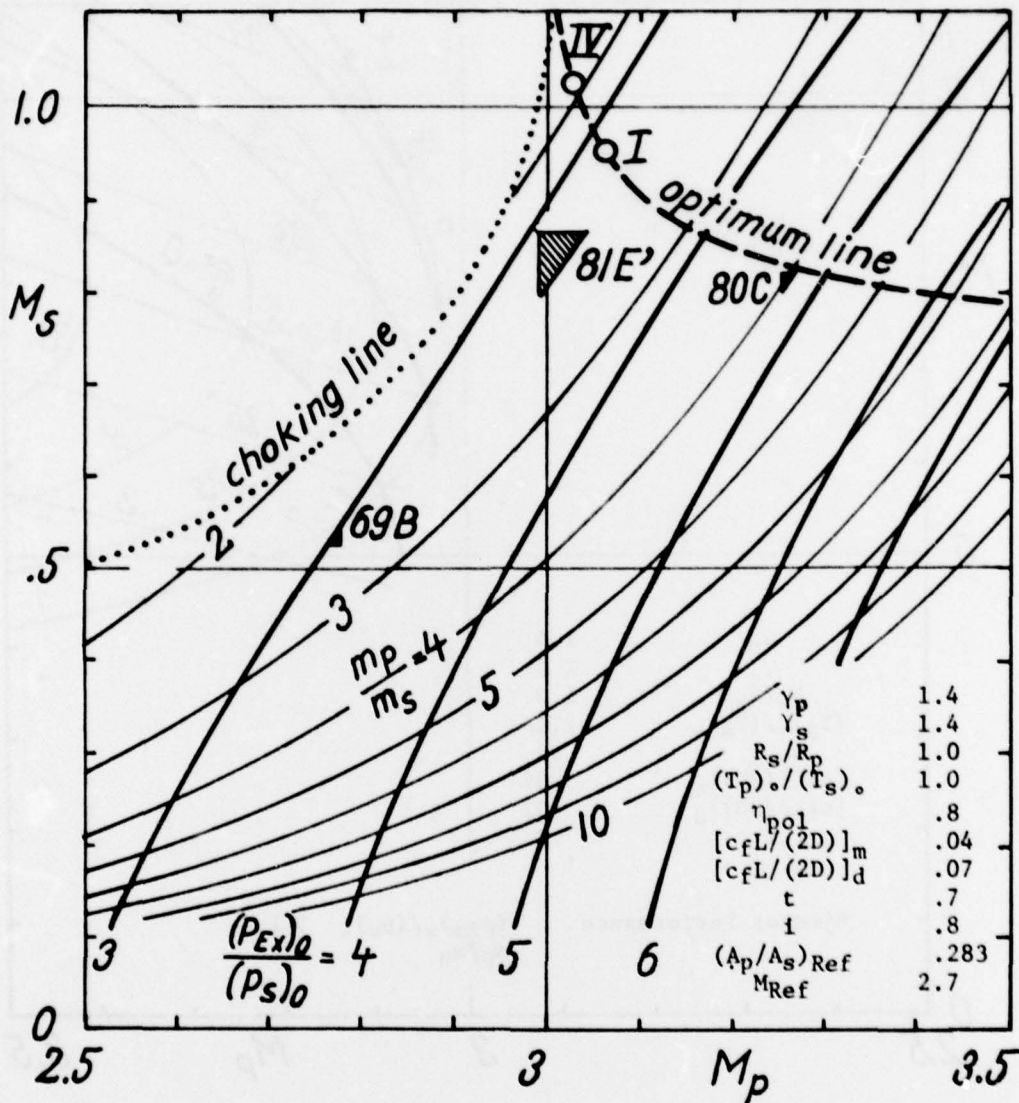


Figure 2. Typical Performance Characteristic of an Ejector with an Ideal Primary Nozzle (nozzle area expansion ratio always adjusted to the operating Mach number). The operating medium for primary and secondary flow is air



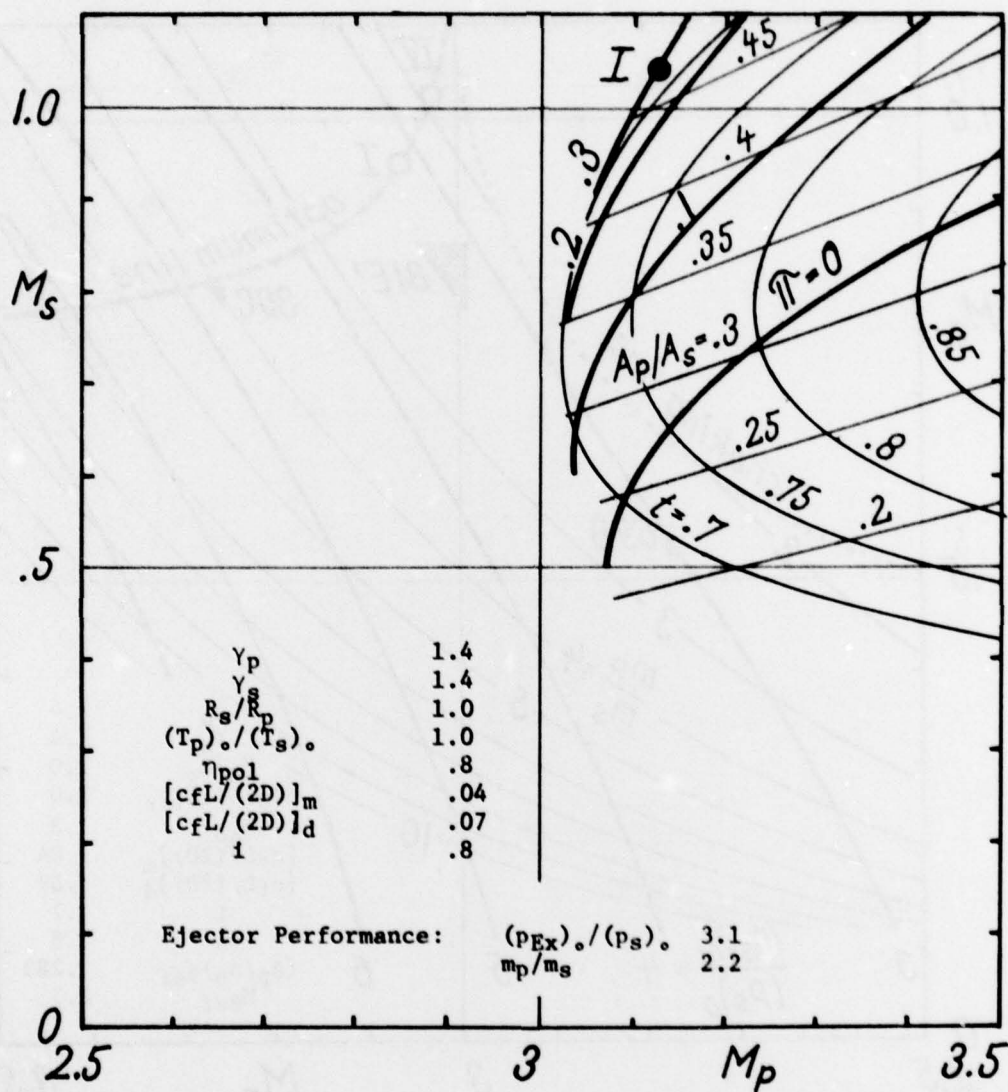


Figure 3. Ejector Optimization, Example I

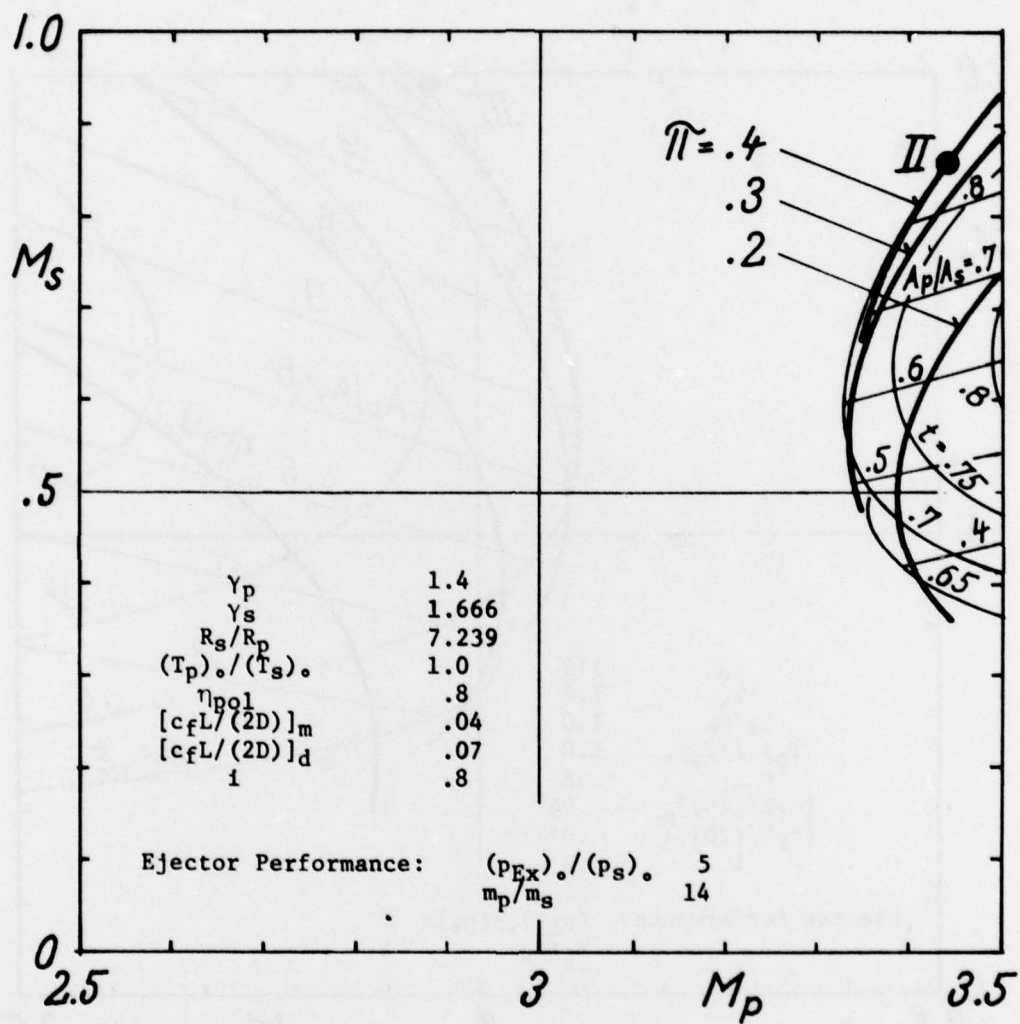


Figure 4. Ejector Optimization, Example II

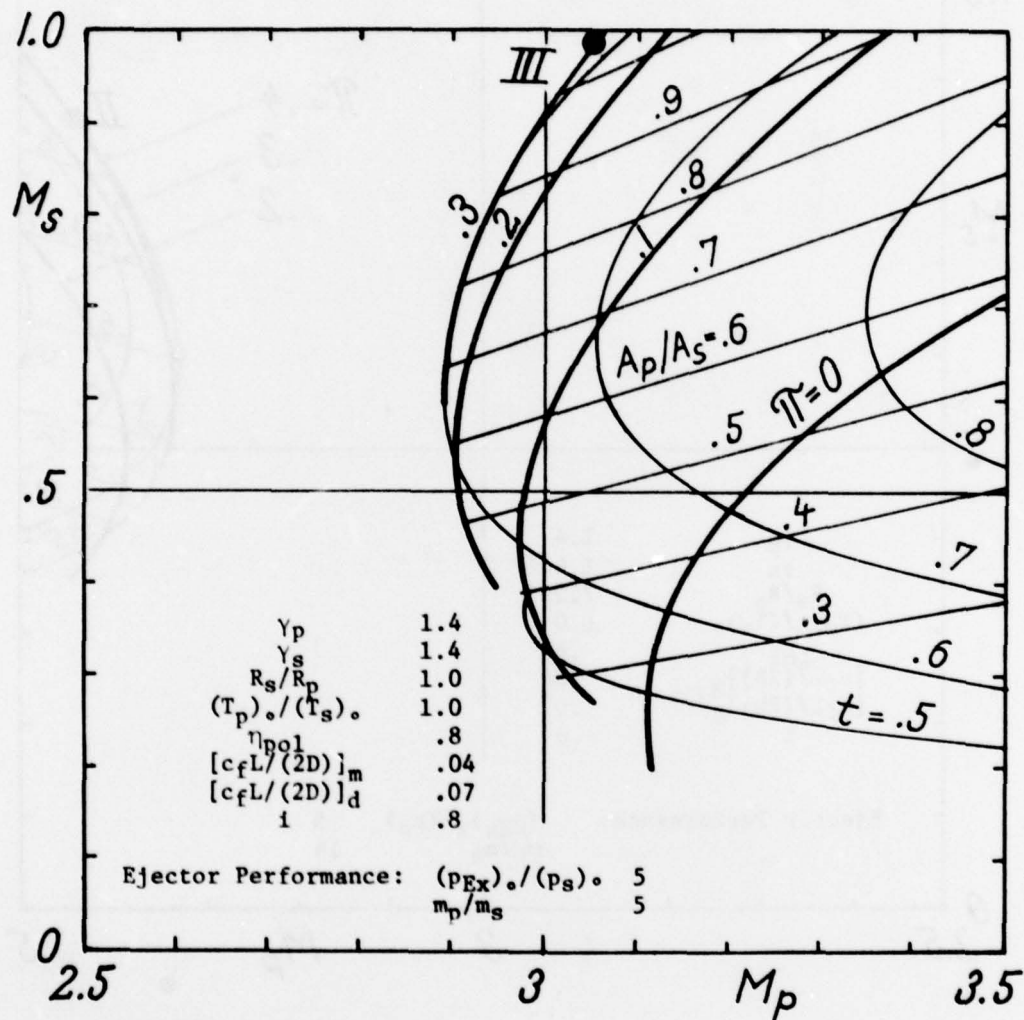


Figure 5. Ejector Optimization, Example III

|       |     |                              |                   |
|-------|-----|------------------------------|-------------------|
| curve | I   | $(p_{Ex})_o / (p_s)_o = 3.1$ | $m_p / m_s = 2.2$ |
|       | II  | 5.0                          | 14.0              |
|       | III | 5.0                          | 5.0               |
|       | IV  | 2.8                          | 2.0               |
|       | V   | 2.5                          | 1.96              |

● approx. point of optimum operation

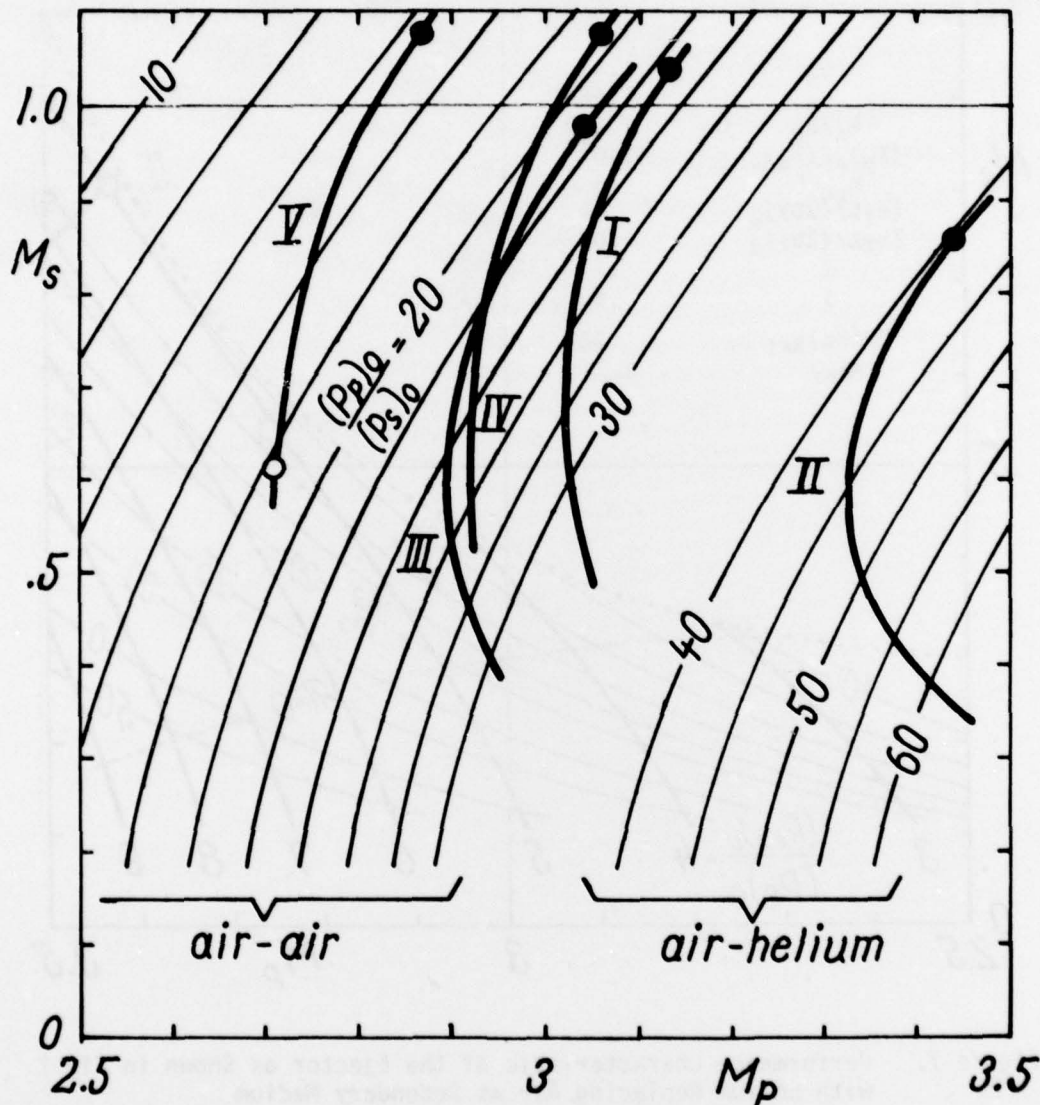


Figure 6. Curves of Constant Total Supply Pressure Ratios (primary to secondary) for Determining the Optimum Operational Point on an Envelope Curve of an Optimization Plot. Five examples of envelope curves are entered. Curves I to III pertain to optimization examples I to III, shown in Figs. 3, 4, and 5, respectively



AFFDL-TR-78-23

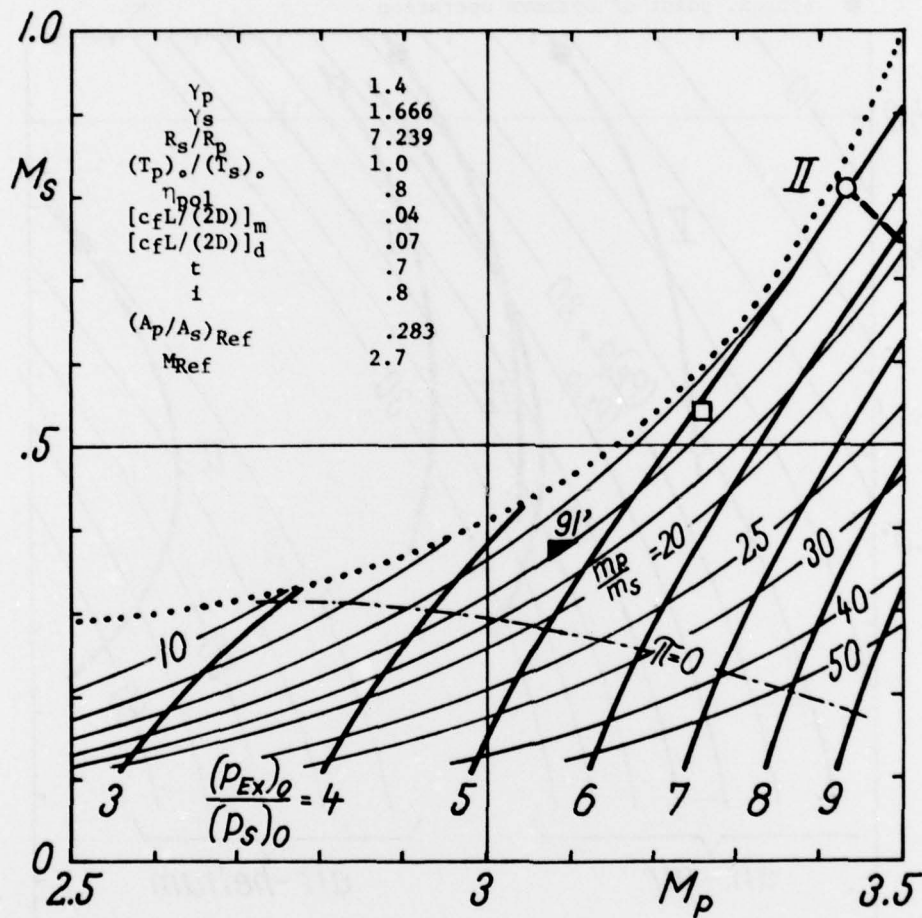


Figure 7. Performance Characteristic of the Ejector as Shown in Fig 2 with Helium Replacing Air as Secondary Medium

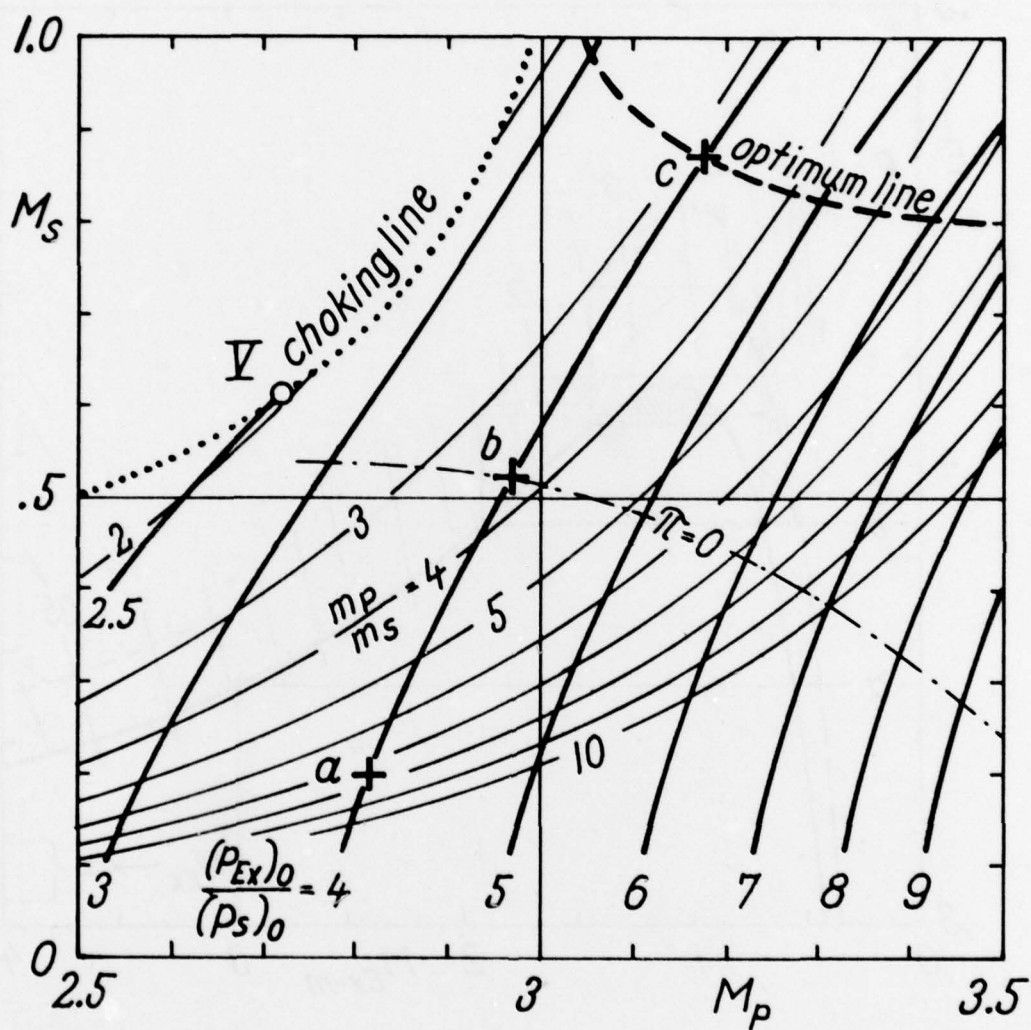


Figure 8. Ejector Performance Characteristic Previously Shown in Fig 2 with Selected Operating Points Marked

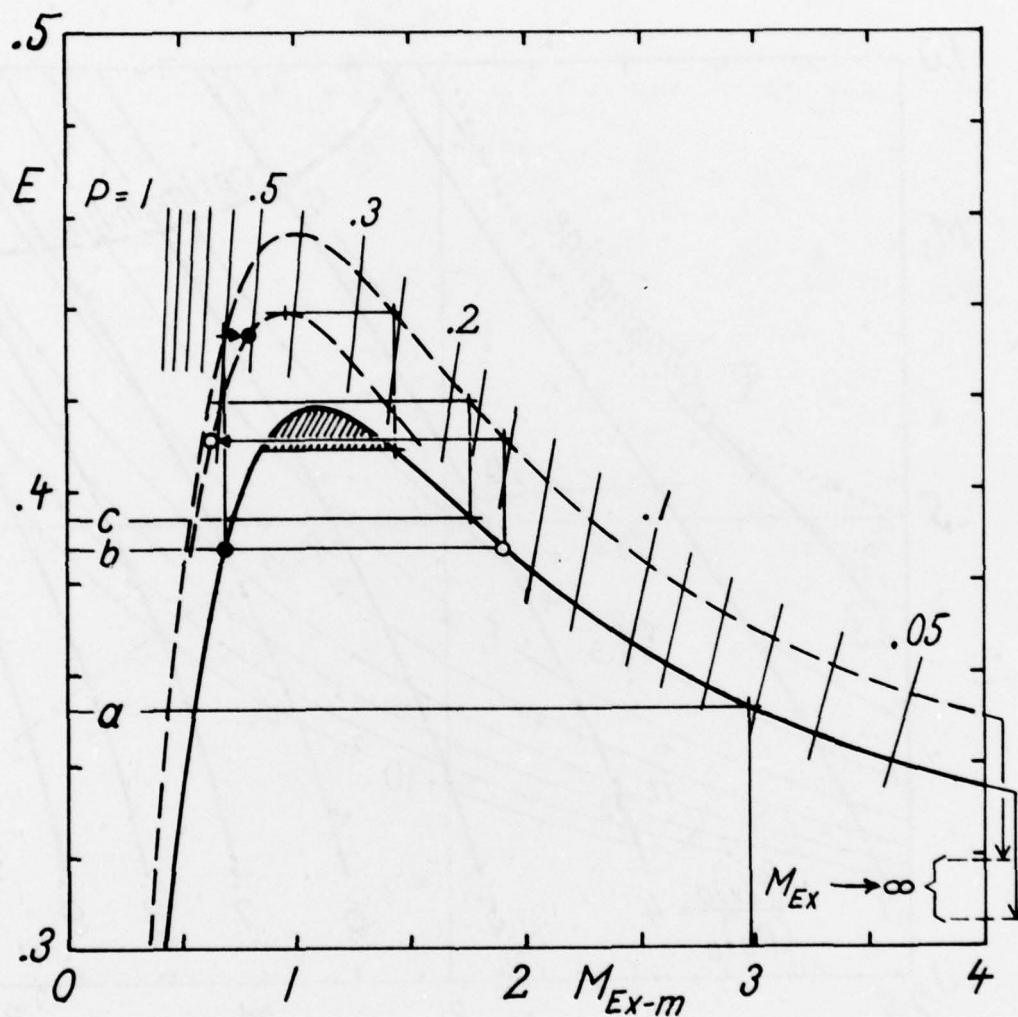


Figure 9. Flow Density Plot for Ejector Conditions Indicated in Fig 2 with Operating Points from Fig 8 Entered